

Full terms and conditions of use: <http://www.tandfonline.com/page/terms-and-conditions>

This article may be used for research, teaching, and private study purposes. Any substantial or systematic reproduction, redistribution, reselling, loan, sub-licensing, systematic supply, or distribution in any form to anyone is expressly forbidden.

The publisher does not give any warranty express or implied or make any representation that the contents will be complete or accurate or up to date. The accuracy of any instructions, formulae, and drug doses should be independently verified with primary sources. The publisher shall not be liable for any loss, actions, claims, proceedings, demand, or costs or damages whatsoever or howsoever caused arising directly or indirectly in connection with or arising out of the use of this material.

## High-Field Torque Magnetometry on Fe<sub>6</sub> and Fe<sub>10</sub> Molecular Magnets

A. CORNIA<sup>a</sup>, A.G.M. JANSEN<sup>b</sup> and M. AFFRONTÉ<sup>c</sup>

<sup>a</sup>*Dipartimento di Chimica, Università di Modena, via G. Campi 183, I-41100 Modena, Italy,* <sup>b</sup>*Grenoble High Magnetic Field Laboratory, CNRS, F-38042 Grenoble CEDEX 9, France and* <sup>c</sup>*INFM and Dipartimento di Fisica, Università di Modena, via G. Campi 216/a, I-41100 Modena, Italy*

We have applied torque magnetometry to the study of magnetic anisotropy in six- and ten-membered rings of iron(III) ions. By using magnetic fields up to 23 Tesla, we have partially overridden the intramolecular antiferromagnetic ordering of the spins ( $J = 20.0 \text{ cm}^{-1}$  and  $9.6 \text{ cm}^{-1}$  in Fe<sub>6</sub> and Fe<sub>10</sub>, respectively) to obtain magnetic ground states with  $S = 1, 2, 3$ , etc.. Torque measurements on microgram single crystals at temperatures down to 0.45 K have shown that spin-flip transitions are accompanied by sharp variations of magnetic anisotropy. The angular dependence of transition fields has provided spectroscopic-quality information about the spin-Hamiltonian parameters in the two compounds. In addition, by analyzing the field dependence of the torque signal we have determined the exchange energies and zero-field splitting parameters of the total-spin multiplets with  $S \leq 5$  in the Fe<sub>10</sub> sample. We conclude that torque magnetometry represents a high-sensitivity, powerful technique for studying field-induced level crossing in molecular magnets.

**Keywords:** iron clusters; high magnetic fields; magnetic anisotropy; torque magnetometry

## INTRODUCTION

Magnetic anisotropy measurements have played a central role in the study of the electronic structure of coordination compounds<sup>[1]</sup>. Recently, renewed interest in this field has arisen from the observation of quantum-size effects in large magnetic clusters at low temperatures. These include quantum tunneling of the magnetization in single-molecule superparamagnets, like  $\text{Mn}_{12}$ <sup>[2]</sup> and  $\text{Fe}_8$ <sup>[3]</sup>, and quantum steps of the magnetization in molecular AFM rings, like  $[\text{NaFe}_6(\text{OCH}_3)_{12}(\text{pmdbm})_6]\text{ClO}_4$  ( $\text{Fe}_6$ )<sup>[4]</sup> and  $[\text{Fe}_{10}(\text{OCH}_3)_{20}(\text{CH}_2\text{ClCO}_2)_{10}]$  ( $\text{Fe}_{10}$ )<sup>[5]</sup>. Large magnetic rings in particular provide the opportunity to observe the coexistence of classical and quantum effects in solid matter. The physical properties of a ring are in fact expected to gradually evolve toward those of a chain as the number of spins increases.  $\text{Fe}_N$  rings with  $N \geq 6$ , for instance, show a critical slowing down of spin fluctuations at temperatures close to  $J/k_B$ , as observed in infinite chains<sup>[6]</sup>. However, M-vs-B curves at  $T \ll 4J/(Nk_B)$  exhibit a regular staircase structure due to quantum-size effects<sup>[4,5]</sup>.

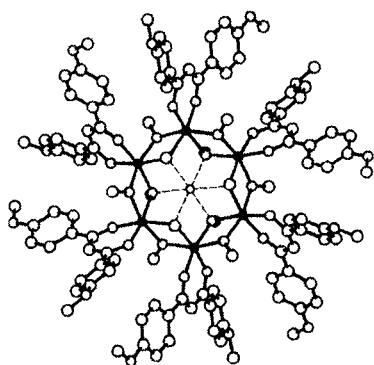


FIGURE 1  
 $[\text{NaFe}_6(\text{OCH}_3)_{12}(\text{pmdbm})_6]^+$

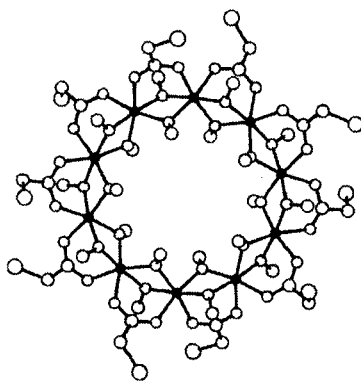


FIGURE 2  
 $[\text{Fe}_{10}(\text{OCH}_3)_{20}(\text{CH}_2\text{ClCO}_2)_{10}]$

This behavior reflects spin-flip transitions induced by the applied magnetic field, which progressively overrides the AFM coupling of the spins. Although the steps rapidly merge into a broad feature as the temperature is increased, the measured width is much larger than expected for simple thermal broadening. Magnetic anisotropy has been invoked to explain the observed width<sup>[4,5]</sup>. In order to confirm this conjecture, we undertook a single-crystal study of quantum-size effects in  $\text{Fe}_6$  (Figure 1) and  $\text{Fe}_{10}$  (Figure 2) by using cantilever torque magnetometry in high fields.

## EXPERIMENTAL

Magnetic fields up to 23 T were applied by using one of the polyhelix electromagnets available at Grenoble High Magnetic Field Laboratory. A high-sensitivity cantilever equipped with a  $^3\text{He}$  cryostat was used for torque experiments on 10- $\mu\text{g}$  single crystals, which were synthesized by literature procedures<sup>[4,5]</sup>. The deflection of the cantilever with respect to the zero-field position was measured by a capacitive method ( $C \propto 1/d$ ). The experimental apparatus (Figure 3) was sensitive to the y-component of the torque vector ( $t_y$ ) acting on the sample in the magnetic field  $B$ , which was applied along the z-axis. In  $\text{Fe}_6$ , the rings are iso-oriented in the

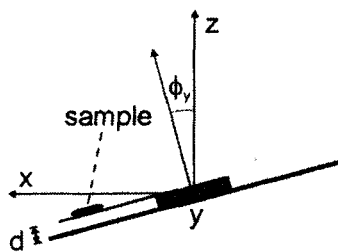


FIGURE 3 Side view of the cantilever torque magnetometer.

crystal (space group  $R\bar{3}$ ) with their six-fold axes lying parallel to the c-axis

(Figure 4a). The b-axis was set parallel to the rotation axis of the goniometer (y), so that the magnetic field was applied in the  $a^*c$  plane at  $\theta = 0-90^\circ$ . In the case of  $\text{Fe}_{10}$  (space-group  $P2_1/c$ ) the situation is slightly more complicated since

each unit cell comprises two rings related by the  $2_1$ -axis and forming a dihedral angle  $2\alpha = 21.1^\circ$  (Figure 4b). The  $b$ -axis was aligned parallel to  $y$  and the magnetic field was applied in the  $ac$  plane with  $\theta$  ranging from  $-10$  to  $95^\circ$ .

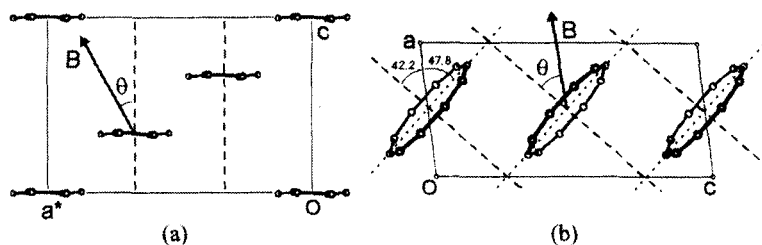


FIGURE 4 (a) Projection of the crystal structure of  $\text{Fe}_6$  onto the  $a^*c$  plane of the rhombohedral unit cell (hexagonal setting). (b) Projection of the crystal structure of  $\text{Fe}_{10}$  onto the  $ac$  plane of the monoclinic unit cell. The traces of six-fold and idealized ten-fold molecular axes are depicted by dashed lines.

## RESULTS

### $\text{Fe}_6$ Sample

Curves recorded at 4.3, 1.4, 0.7 and 0.45 K for  $\theta = 45^\circ$  show a sharp, step-like decrease of the capacitance with increasing  $B$  (Figure 5). Since the capacitance variation is simply proportional to  $t_y$ , it follows that  $t_y < 0$ . This directly provides the sign of magnetic anisotropy, pointing to the presence of a hard magnetic axis along  $c$ . Although the inflection point of the steps ( $B_c$ ) is the same at all temperatures, the full-width-at-half-maximum (FWHM) increases from 1.56 T at 0.45 K to about 12.3 T at 4.3 K (inset in Figure 5). For  $T < 1$  K, however, the FWHM is small enough to reveal a smooth shift of  $B_c$  as a function of  $\theta$  (Figures 6-7). In particular, when  $B$  is virtually parallel to the  $c$ -axis the step occurs at higher fields (17.9 T) as compared to the perpendicular orientation

(15.4 T). Furthermore, the torque signal vanishes when  $\theta$  is close to 0 and  $90^\circ$  which represent principal directions of magnetic susceptibility<sup>[1]</sup>.

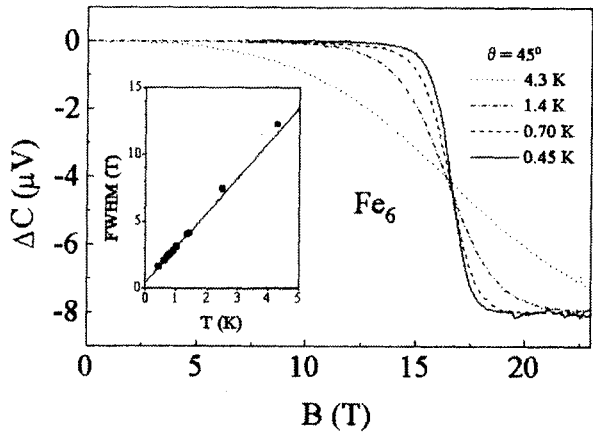


FIGURE 5 Torque curves measured on the  $\text{Fe}_6$  sample as a function of temperature at  $\theta = 45^\circ$ . The inset shows the temperature dependence of the FWHM for the step.

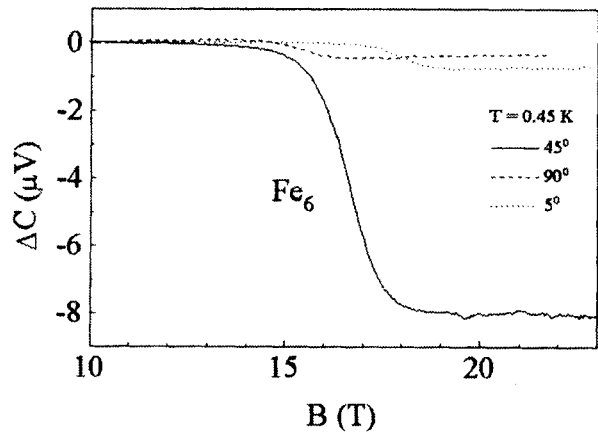


FIGURE 6 Torque curves measured on the  $\text{Fe}_6$  sample at 0.45 K.

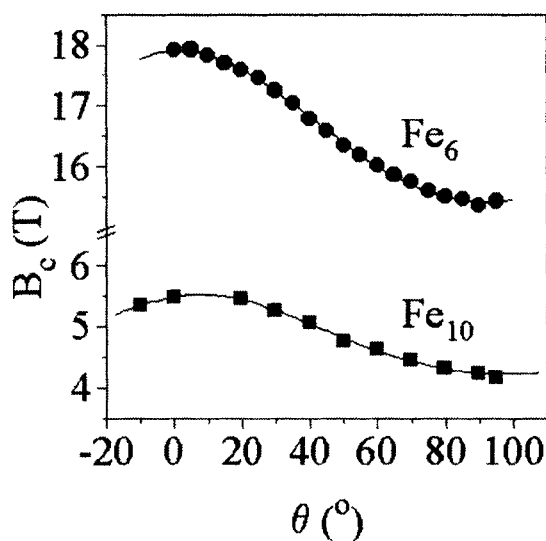


FIGURE 7  $B_c(\theta)$ -vs- $\theta$  plot for the first magnetization step.

### **Fe<sub>10</sub> Sample**

In the torque curve recorded at 0.45 K and  $\theta = 49.8^\circ$ , four steps centered at 4.8, 9.2, 13.6 and 18.0 T can be clearly resolved (Figure 8). The steps have similar width among each other and their FWHM (1.6 T) is comparable with that found in the six-membered ring at the same temperature (1.56 T). The steps rapidly merge into a broad feature as the temperature is increased above 1 K (Figure 8). From the sign of  $\Delta C$  we conclude that the crystal tends to rotate so as to increase the  $\theta$  angle (See Figure 4b). We observed vanishingly small torque signals for  $\theta$  close to 0 and  $90^\circ$ , which must therefore correspond to principal magnetic directions in the ac plane. The pattern of  $B_c$  values for the first step is plotted in Figure 7 and looks quite similar to that found in the  $Fe_6$  sample, with critical fields in the range 5.6-4.2 T.



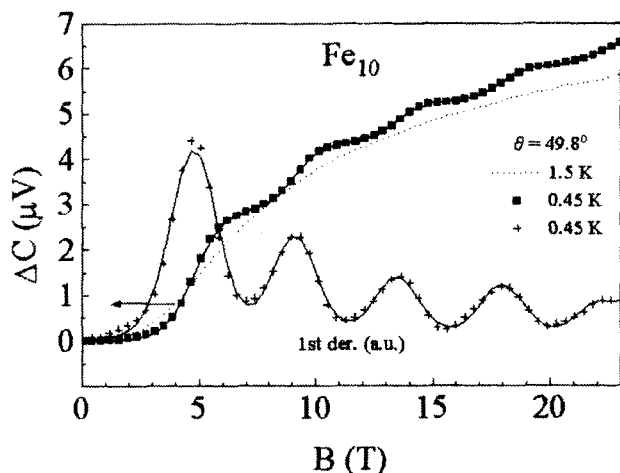


FIGURE 8 Torque curves measured on the  $\text{Fe}_{10}$  sample at  $\theta = 49.8^\circ$ . The solid line gives the best fit to the 0.45-K data. The first derivatives of experimental and calculated curves are also shown in arbitrary units.

## DISCUSSION

In low magnetic fields,  $\text{Fe}_6$  and  $\text{Fe}_{10}$  have a nonmagnetic  $S = 0$  ground state due to dominant n.n. Heisenberg interactions:

$$\mathbf{H} = J \sum_{i=1}^N \mathbf{S}_i \cdot \mathbf{S}_{i+1}$$

with  $J = 20 \text{ cm}^{-1}$  and  $9.6 \text{ cm}^{-1}$  in the two compounds, respectively. However, the ground state becomes magnetic in high fields. Quantum steps in  $M$ -vs- $B$  curves at  $T < 1 \text{ K}$  give a clear picture of the progressive, step-wise decoupling of the spins with increasing  $B$ [4,5]. Since the different multiplets may have different anisotropies, level crossing should in general give rise to steps in the torque signal as well.

For simplicity, we will restrict ourselves to the strong-exchange regime while analyzing the singlet-triplet crossing in detail (Figure 9). Since the  $S = 0$  state (0) is magnetically isotropic, the torque signal must reflect contributions from the triplet state (1) only. At each  $\theta$  value, we can safely assume a linear field-dependence of the triplet level (1) around the crossing

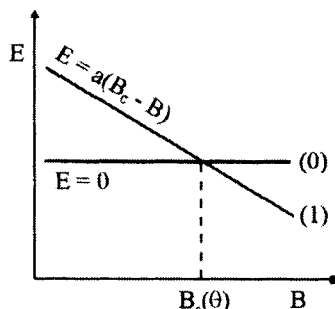


FIGURE 9

point  $B_c(\theta)$ , so that the thermal expectation value of  $t_y$  is given by:

$$\langle t_y \rangle = \langle 1 | T_y | 1 \rangle \left[ 1 + \exp \left( -a \frac{B - B_c(\theta)}{k_B T} \right) \right]^{-1}$$

where  $-a$  is the slope of (1) at  $B_c(\theta)$  and

$$T_y = - \left( \frac{\partial H}{\partial \theta} \right)_B$$

is the torque operator. It can be shown that

$$\text{FWHM} = \left( \frac{k_B T}{a} \right) \ln \left( \frac{3 + 2\sqrt{2}}{3 - 2\sqrt{2}} \right)$$

for the step, which is centered at the critical field  $B_c(\theta)$ .

The FWHM-vs-T data at  $T < 1.5$  K in Figure 5 were fitted with  $a = 0.932(11)$   $\text{cm}^{-1}/\text{T}$ . This value is in excellent agreement with that expected for singlet-triplet crossing ( $a = -g\mu_B M = 0.934$   $\text{cm}^{-1}/\text{T}$  with  $g = 2.00$ ). We now assume axial symmetry for both systems investigated and express the critical field as:

$$B_c(\theta) = \frac{E_1 + \frac{1}{3}D_1}{g\mu_B} \left\{ \frac{E_1 - \frac{2}{3}D_1}{E_1 + \frac{1}{3}D_1 [1 - 3\cos^2(\theta' - \theta_0)]} \right\}^{\frac{1}{2}}$$

with  $\theta' = \theta$  in  $\text{Fe}_6$  and  $\theta' = \arccos(\cos\alpha\cos\theta)$  in  $\text{Fe}_{10}$  (see Experimental Section).

$E_1$  and  $D_1$  are the exchange energy and the axial zero-field splitting parameter, respectively, for the triplet state. The  $\theta_0$  angle defines the orientation of the anisotropy axis in the xz plane. This Equation provides a simple and efficient way for determining  $E_1$  and  $D_1$  from  $B_c(\theta)$ -vs- $\theta$  plots (Figure 7). The best-fit parameters are collected in Table I.

TABLE I

	$\text{Fe}_6$	$\text{Fe}_{10}$
$E_1$ ( $\text{cm}^{-1}$ )	15.28(1)	4.479(4)
$D_1$ ( $\text{cm}^{-1}$ )	4.32(3)	2.24(2)
$\theta_0$ ( $^\circ$ )	-1.6(4)	7.7(1)
$g$	2.000	2.000

TABLE II

S	$E_S$ ( $\text{cm}^{-1}$ )	$D_S$ ( $\text{cm}^{-1}$ )
1	4.43(1)	2.24
2	12.78(3)	0.599(3)
3	25.28(5)	0.291(1)
4	41.98(8)	0.180(1)
5	62.6(2)	0.123(1)

The  $\theta_0$  value for  $\text{Fe}_{10}$  shows that the axial approximation is realistic, as suggested by a careful inspection of molecular geometry<sup>[5]</sup>.

The additional steps observed in high fields on the  $\text{Fe}_{10}$  sample were analyzed by including excited multiplets with S up to 5. Our approach consisted in directly fitting the  $t_y$ -vs-B curve recorded at 0.45 K and  $\theta = 49.8^\circ$ , which showed best-resolved steps and maximum signal intensity. The eigenvectors of perturbative hamiltonians  $\mathbf{H}_S = \mathbf{S} \cdot \mathbf{D}_S \cdot \mathbf{S} + g\mu_B \mathbf{B} \cdot \mathbf{S}$  were computed for each S-multiplet and the thermal-expectation value of the torque signal was calculated from the matrix elements  $\langle \text{SM} | \mathbf{T}_y | \text{SM} \rangle$  by using Boltzmann statistics. The best-fit parameters in Table II were obtained by setting  $D_1 = 2.24$ ,  $g = 2.00$  and refining an "effective temperature"  $T' = 0.76(1)$  K in order to reproduce the width of the steps. Tables I and II provide a detailed picture of low-lying spin states in these AFM clusters. The possibility to determine the complete set of exchange energies and zero-field splitting parameters reflects the different influence of  $D_S$  and  $E_S$  on the torque curves. More precisely, the height of each

step is mainly determined by the  $D_S/D_{S+1}$  ratio, whereas the inflection point is related to both  $D_S$  and  $E_S$  values.

## CONCLUDING REMARKS

We have investigated the influence of non-Heisenberg terms on the low-temperature physics of two molecular clusters with a ring structure,  $\text{Fe}_6$  and  $\text{Fe}_{10}$ . Torque magnetometry on microgram single crystals was applied to the study of magnetization steps in fields up to 23 Tesla. The smooth angular variation of critical fields provided a very effective way of determining the  $D_S$  parameters and the exchange energies of excited multiplets. The main advantage of this approach, as compared to low-field susceptibility measurements at variable temperature, lies in the absence of thermal averaging effects on the different multiplets, which mix individual contributions to magnetic anisotropy. In this respect, the information extracted from single-crystal magnetization steps is “quasi-spectroscopic” in quality.

In both  $\text{Fe}_6$  and  $\text{Fe}_{10}$  compounds, the ring axis represents a “hard” magnetic axis. This result is surprising if one considers the different chemical environment of the metal ions in the clusters. However, it has found recent confirmation by torque measurements on two additional ring clusters, namely  $[\text{LiFe}_6(\text{OCH}_3)_{12}(\text{dbm})_6]\text{PF}_6$ <sup>[7,8]</sup> and  $[\text{Fe}_8\text{F}_8(\text{t-BuCO}_2)_{16}]$ <sup>[8]</sup>. The zero-field splitting parameters observed in  $\text{Fe}_6$  and  $\text{Fe}_{10}$  confirm that polynuclear iron(III) compounds may exhibit fairly large magnetic anisotropies and represent good candidates for the observation of superparamagnetic-like behavior<sup>[3]</sup>.

## Acknowledgments

The authors thank Prof. Dante Gatteschi for invaluable discussion and Dr. Andrea Caneschi for providing the  $\text{Fe}_{10}$  sample.

## References

- [1] (a) W. De W. Horrocks, jr., and D. De W. Hall, *Coord. Chem. Rev.*, **6**, 147 (1971). (b) S. Mitra, *Prog. Inorg. Chem.*, **22**, 309 (1977).
- [2] (a) C. Paulsen, J.-G. Park, B. Barbara, R. Sessoli, and A. Caneschi, *J. Magn. Magn. Mater.*, **140**, 1891 (1995). (b) L. Thomas, F. Lioni, R. Ballou, D. Gatteschi, R. Sessoli, and B. Barbara, *Nature*, **383**, 145 (1996). (c) J. R. Friedman, M. P. Sarachik, J. Tejada, J. Maciejewski, and R. Ziolo, *Phys. Rev. Lett.*, **76**, 3820 (1996).
- [3] (a) A.-L. Barra, P. Debrunner, D. Gatteschi, C. E. Schulz, and R. Sessoli, *Europhys. Lett.*, **35**, 133 (1996). (b) C. Sangregorio, T. Ohm, C. Paulsen, R. Sessoli, and D. Gatteschi, *Phys. Rev. Lett.*, **78**, 4645 (1998).
- [4] A. Caneschi, A. Cornia, A. C. Fabretti, S. Foner, D. Gatteschi, R. Grandi, and L. Schenetti, *Chem. Eur. J.*, **2**, 1379 (1996).
- [5] K. L. Taft, C. D. Delfs, G. C. Papaefthymiou, S. Foner, D. Gatteschi, and S. J. Lippard, *J. Am. Chem. Soc.*, **116**, 823 (1994).
- [6] (a) A. Lascialfari, Z. H. Jang, F. Borsa, D. Gatteschi, and A. Cornia, *J. Appl. Phys.*, **83**, 6946 (1998). (b) A. Lascialfari, D. Gatteschi, A. Cornia, U. Balucani, M. G. Pini, and A. Rettori, *Phys. Rev. B*, **57**, 1115 (1998). (c) A. Lascialfari, D. Gatteschi, F. Borsa, and A. Cornia, *Phys. Rev. B*, **55**, 14341 (1997).
- [7] G. L. Abbati, A. Cornia, A. C. Fabretti, W. Malavasi, L. Schenetti, A. Caneschi, and D. Gatteschi *Inorg. Chem.*, **36**, 6443 (1997).
- [8] A. Cornia, E. Rentschler, A. G. M. Jansen, and M. Affronte, to be published.